Analysis of front interaction and control in stationary patterns of reaction-diffusion systems

Moshe Sheintuch* and Olga Nekhamkina
Department of Chemical Engineering, Technion–Israel Institute of Technology, Haifa, Israel 32000
(Received 21 November 2000; published 24 April 2001)

We have analyzed the stability of one-dimensional patterns in one- or two-variable reaction-diffusion systems, by analyzing the interaction between adjacent fronts and between fronts and the boundaries in bounded systems. We have used model reduction to a presentation that follows the front positions while using approximate expressions for front velocities, in order to study various control modes in such systems. These results were corroborated by a few numerical experiments. A stationary single front or a pattern with *n* fronts is typically unstable due to the interaction between fronts. The two simplest control modes, global control and point-sensor control (pinning), will arrest a front in a single-variable problem since both control modes, in fact, respond to the front position. In a two-variable system incorporating a localized inhibitor, in the domain of bistable kinetics, global control may stabilize a single front only in short systems while point-sensor control can arrest such a front in any system size. Neither of these control modes can stabilize an *n*-front pattern, in either one- or two-variable systems, and that task calls for a distributed actuator. A single space-dependent actuator that is spatially qualitatively similar to the patterned setpoint, and which responds to the sum of deviations in front positions, may stabilize a pattern that approximates the desired state. The deviation between the two may be sufficiently small to render the obtained state satisfactory. An extension of these results to diffusion-convection-reaction systems are outlined.

DOI: 10.1103/PhysRevE.63.056120 PACS number(s): 82.40.Ck, 05.45.−a

I. INTRODUCTION

The problem of finite-dimensional control of systems that are described by partial-differential equations (PDE) has been attracting considerable attention, especially for applications of reaction and diffusion [1–4] and fluid-flow processes [5]. The traditional approach in chemical engineering problems of control is to use a finite, preferably small, discretization of the underlying PDE [6,7]. Sharp spatial variations in the state variable make the use of large discretization models unavoidable. The dissipative nature of the underlying PDEs and numerous studies of the spectrum of the eigenvalues of the linearized system suggest that the long term dynamics is low dimensional. Several approaches for model reduction have been suggested; recent approaches were based on the central manifold theorem [8,2]. While these approaches may be powerful, they do not support any qualitative understanding of the system behavior to suggest efficient modes of control.

Stationary fronts are key elements in the emergence of stationary or moving patterns and following their motion is a natural approach for model reduction. Various mechanisms have been suggested for the emergence of stationary patterns in reaction-diffusion systems, and some are reviewed below. While analytical results exist for a single front in unbounded systems [9,10], the behavior of a realistic bounded (*finite-size*) system with several fronts cannot be predicted analytically in most cases; moreover, numerical simulations are tedious as front motion and front interaction is extremely slow.

The purpose of this work is to derive approximate solutions for the stability and dynamics of stationary patterns, in a bounded one-dimensional reaction-diffusion system, and apply them in various control procedures. The stability analysis is based on model reduction to a model for front positions and on approximate solutions of front velocity and of front interaction under conditions where separations between fronts is finite. Our interest in the control of these systems stems from the novelty of the problem and from our expectations that control methodologies developed for diffusion-reaction systems may be applied for certain control problems that arise in diffusion-convection-reaction systems [11], as we comment in the conclusion of this work. The patterns emerge or are destroyed due to the interaction of the activator (x) with various control modes (λ) or various inhibitors (y). The activator, typically described by the reaction-diffusion equation

$$x_t - x_{zz} = f(x,y) + \lambda, \quad x_z|_0 = x_z|_L = 0, \tag{1a}$$

may admit front solution when the source function $(f(x,y) + \lambda = 0)$ is bistable. We verify that a single stationary front or a pattern of several stationary fronts of system (1a) is generically unstable due to front interaction. We then study various stabilizing and destabilizing effects and approximate the boundaries of existence of such fronts and patterns under these conditions.

The destabilizing forces we address are due to front interaction or due to an inhibitor (y), which is localized and slow $(\varepsilon \ll 1)$, which typically accounts for oscillatory kinetics in high- and low-pressure catalytic systems [12]. Its description is as follows:

$$y_t = \varepsilon g(x,y). \tag{1b}$$

Reaction-diffusion systems with a localized inhibitor [i.e., Eq. (1)] may admit stationary front solutions, when $f(x,y) + \lambda = g(x,y) = 0$ is bistable, but these are highly unstable.

*Corresponding author. Email address: cermsll@tx.technion.ac.il

Stabilizing effects can be imposed by external control or by long-ranged inhibitors, as described in the following.

(i) Instantaneous global interaction or global control, in which the actuator responds to deviations of the spatially averaged sensor like

$$\lambda = B(x_s - \langle x \rangle), \tag{2}$$

where $\langle \ \rangle$ denotes the spatial average and x_s is the desired setpoint, may stabilize a single front. In that case the setpoint is a parameter and with large B the system instantaneously adjusts its λ to satisfy the setpoint. A strong interaction in a long system will eliminate an unstable homogeneous solution. That implies that a fixed part of the surface (half in the symmetric case) lies in the upper state. Patterns due to such interaction were analyzed and simulated to account for observations of patterns in electrochemical systems [13], in catalytic wires or ribbons controlled to maintain a constant resistance [14,15], in catalytic disks suspended in a well-mixed fluid phase and in dc-discharge systems (see [12] for a recent review of catalytic systems). Global interaction in chemical reactors may be induced by convection or by mixing of the reactant fluid phase.

(ii) In the limit of infinite gain ($B \to \infty$) the global-interaction condition may be incorporated into the original equation, by integrating Eq. (1a) and expressing λ, to form an integrodifferential equation of the form $x_t - x_{zz} = f(x,y) - \langle f(x,y) \rangle$; $\langle x \rangle = x_s$.

Equations (1) and (2) have been extensively investigated as a model of the catalytic oscillator subject to global interaction or global control. We test here the efficiency of global control for stabilizing desired patterns. We mention below three other mechanisms that may lead to stationary patterns but we do not employ them here: In a system with nonuniform properties, $\lambda(z)$, gradients in λ may arrest a front of an opposite inclination and a periodic $\lambda(z)$ may stabilize a stationary multifront pattern. In the classical Turing mechanism patterns emerge when the activator (x) is short-ranged while the inhibitor's (λ) diffusivity is sufficiently large to arrest the propagation of fronts of the activator. Other mechanisms involve convection [16] and the behavior of such a system will be studied elsewhere.

We are looking now to design a controller of system (1) with as few sensors as possible and possibly with a single actuator. While continuous measurements of the spatial state-variable (e.g., temperature) profile may be possible in certain cases, it is still technically challenging in most cases and we rely on localized sensors or on average properties. The controller we design is of the form

$$\lambda - \lambda^* = BA[x(t)]\psi(z). \tag{3}$$

Technically it implies that $\psi(z)$ should be constructed once in the required space-dependent shape. In chemical reactors this can be implemented by installing spatially varying resistance if resistive heating is employed, or by varying the heat-transfer area when heat exchange is employed.

We will consider uniforms and space-dependent actuators. We consider first the simplest controller structure, a space independent actuator $\psi = 1$. The simplest controller should be based on a single measurement. *Global control*, $A(t) = x_s - \langle x \rangle$, is based on certain average property, as discussed above. In a *point-sensor* control x is measured at a single point Z^*, preferably at the front position, $A(t) = x_s(Z^*) - x(Z^*)$. This control mode is sometimes referred to as *pinning*. In a single-front pattern, and for small deviations, the two control modes actually respond to the front position, as we show below in the analysis of the two strategies. We then turn to study space-dependent actuators, where we try to stabilize a certain pattern with a qualitatively similar actuator.

We employ below the simplest oscillatory kinetics model, i.e., a cubic activator source function

$$f = -x^3 + x + y$$

coupled with a linear balance on the inhibitor $(g(x,y))$. Many of the numerical and analytical studies of patterns due to long-range interaction typically employed such kinetics [14,17–20] and showed that patterns simulated with a realistic model, using a bistable activator kinetic balance and a monotonic inhibitor balance [15], were quite similar to those obtained with the cubic kinetics. The advantages gained by analyzing this simple model is that it obeys certain symmetries, which will be employed for pattern classification, and that several of its asymptotes, including the fixed λ case, have been analyzed before for one- or two-dimensional systems [18].

The structure of this work is the following: In Sec. II we derive an approximate solution for front velocity in a bounded system and then use it to study the stability of patterns with one, two, or any number of fronts of the single-variable problem [Eq. 1(a)] without or with various stabilizing modes. In this section we consider the two control strategies with a uniform actuator. Control strategies for stabilizing multifront patterns are implemented in Sec. III; specifically we try to develop a methodology that uses a single space-dependent actuator and as few and as simple sensors as possible. In Sec. IV we introduce the slow and localized inhibitor (y) and study its effects and the relevant control procedures.

II. FRONT INTERACTION (SINGLE VARIABLE)

While certain analytical and approximate results exist for the velocity of fronts in systems of the form $x_t - x_{zz} = f(x,\lambda)$, these apply typically for an unbounded (infinitely long) system with fixed coefficients (λ). Since we are interested in the behavior of finite-size systems, and in systems where the distance between adjacent fronts is not too large, we review now the correction to front velocity.

In a frame of a coordinate moving with the front,

$$u = z - ct,$$

the system is described by

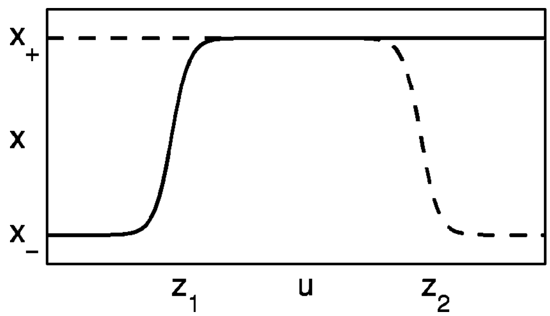

FIG. 1. Front interaction in a finite domain: the figure shows one front (solid line) at Z_1 and another imaginary mirror-imaged one (broken line) at Z_2 (dimensionless variables and parameters).

$$-cx_u - x_{uu} = f(x,\lambda). \tag{4}$$

If c_∞ is the front velocity in an infinitely long system and x_-, x_+ are the stable solutions of $f(x,\lambda)=0$, which are also the edge states in an unbound system, then after multiplying Eq. (4) by x_u and integrating we find

$$-c_\infty \int_{-\infty}^{+\infty} x_u^2 du - \frac{1}{2} x_u^2 \Big|_{-\infty}^{\infty} = \int_{x_-}^{x_+} f(x,\lambda) dx. \tag{5}$$

For the derivation below we impose no-flux conditions at the boundaries and the second term in the equation above is zero. Analytical expressions exist in a few cases only, but let us assume that the front is at Z and its shape is described by $x = x_\infty(u-Z)$.

Strictly speaking, fronts of constant speed and shape do not exist in bounded systems, but we assume the system to be sufficiently large. Now, to find the interaction between two fronts, or similarly the interaction with the walls, where no-flux conditions apply, let assume the existence of two fronts, one at $z=Z_1$ separating a ''cold'' zone on the left from a ''hot'' one and another, its mirror image, at Z_2 (Fig. 1). The corresponding solutions, in the absence of a second front, would have been $x_1 = x_\infty(u-Z_1)$ and $x_2 = x_\infty(Z_2 - u)$. A reasonable approximation of a pulse composed of two mirror-image fronts, is

$$x(u) = x_1(u;Z_1) + [x_2(u;Z_2) - x_+] \tag{6}$$

since it describes correctly each front individually, as their separation diverges to infinity. Without loss of generality let us place the fronts at $Z_1 = -Z_2$, so that $x(u)$ acquires its maximum at $u=0$ due to symmetry. We can integrate now Eq. (4) from $-\infty$ to 0. Substituting $x(u)$ from Eq. (6) and treating the correction as a perturbation and expanding the right-hand side of Eq. (4), as $f(x) = f(x_1) + f_x(x_1)[x_2(u) - x_+]$, which is valid in the vicinity of Z_1, we can substitute $x(u)$ into Eq. (5) and find

$$\begin{aligned} -c \int_{-\infty}^{0} x_u^2 du - \frac{1}{2} x_u^2 \Big|_{-\infty}^{0} &= \int_{-\infty}^{0} f(x,\lambda) \frac{dx}{du} du \sim \int_{-\infty}^{0} f(x_1,\lambda) \frac{dx_1}{du} du \\ &+ \int_{-\infty}^{0} \frac{df}{dx}(x_1,\lambda)[x_2 - x_+] \frac{dx_1}{du} du \\ &+ \int_{-\infty}^{0} f(x_1,\lambda) \frac{dx_2}{du} du. \end{aligned} \tag{7}$$

Now, for conditions where $c_\infty = 0$ the right-hand side can be calculated if the profile is known (as we show below for a cubic f). The first term on the left can be approximated with $x_1(u)$, since $\langle x_{1u}^2 \rangle$ is positive and the correction due to x_2 is small. Otherwise, the right-hand side can be approximated as

$$-c\langle x_u^2 \rangle = f_x(x_+)[x_1(0) - x_+][x_2(0) + x_1(0)/2 - 3x_+/2]. \tag{8}$$

When the front profile is not known we note that far from the front the profile approaches asymptotically the steady solutions of $f(x,\lambda)=0$ as

$$\begin{aligned} &u - Z_1 \to \infty, \quad (x_+ - x) = C_+ \exp[-p_+(u - Z_1)], \\ &2p_+ = c + \sqrt{c^2 - 4f_x(x_+)}, \\ &u - Z_1 \to -\infty, \quad (x - x_-) = C_- \exp[p_-(u - Z_1)], \\ &2p_- = -c + \sqrt{c^2 - 4f_x(x_-)}, \end{aligned} \tag{9}$$

where p_- and $-p_+ < 0$ are the eigenvalues of Eq. (4) at the two stable states (x_- and x_+). Now, for the symmetry assumed for the two fronts, $x_2(z) = x_1(-z)$, $C_+ = C_-$. Consequently, $x_+ - x_1(0) = C_+ \exp(p_+ Z_1) = x_+ - x_2(0)$ (recall that $Z_1 < 0$), and

$$c \sim -C_+^2 \frac{3f_x(x_+)}{2\langle x_u^2 \rangle} e^{-2p_+ Z_1}. \tag{10}$$

Thus, in the general multifront case the velocity of an ascending front Eq. (10) can be generalized to account for interactions on the left and the right

$$c - c_\infty = \alpha_- e^{-2p_- Z_l} - \alpha_+ e^{-2p_+ Z_r}, \tag{11}$$

where Z_l Z_r are the distances (in absolute value) to the closest boundaries on the left and right, respectively. When another front exists on the left or the right than $Z_{l,r}$ is half the distance between the fronts.

A. Approximate front profile

For the simple cubic $f = -x^3 + x + \lambda$ that we use below, and around $\lambda = 0$, conditions at which the front is stationary in an infinitly long system ($c_\infty = 0$),

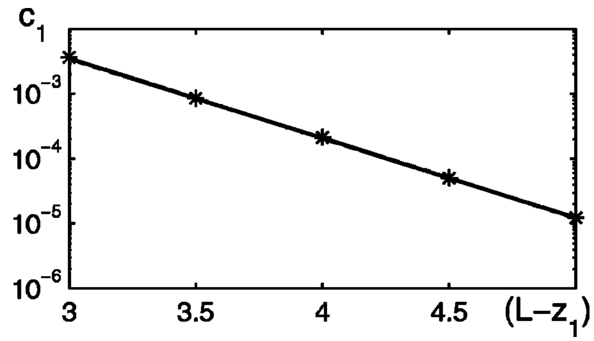

FIG. 2. Comparison of simulated (stars) and approximated (solid line) front velocity as a function from its distance from the boundary (single-variable system, $L=20$; dimensionless variables and parameters).

$$x_\infty = \pm \tanh \frac{u-Z}{\sqrt{2}}, \quad x_1 = \tanh \frac{u-Z_1}{\sqrt{2}}, \quad x_2 = \tanh \frac{Z_2-u}{\sqrt{2}}. \tag{12}$$

The velocity for the two fronts situation described above is obtained by substitution in Eq. (10), yielding for the velocity of the first front

$$-c_1 = \frac{24}{\sqrt{2}} e^{-(Z_2-Z_1)\sqrt{2}} \tag{13}$$

while $c_2 = c_1$ due to symmetry. A rigorous derivation of this expression can be found in [21]. To test this expression we simulated the motion of a front in a bounded system (of size $L=20$) and calculated its velocity (at the inflection point) as the distance from the edge is varying, showing excellent agreement with Eq. (13) (Fig. 2). For the present case, $f_x(x_-) = f_x(x_+) = -2$ and from Eq. (9) $p_\pm^2 \sim (-4f_x)/4 = 2$ where we assumed that $c \ll f_x$ (recall that $c_\infty = 0$ at $\lambda = 0$); thus, $\alpha_- = \alpha_+ = \alpha$, $p_- = p_+ = p$.

The velocity of front solutions of Eq. (1a) with $f = (x_+ - x)(x - x_i)(x - x_-)$, in an infinitely long system, is

$$c_\infty = (x_+ + x_- - 2x_i)/\sqrt{2},$$

(see [10]). The upper and lower branches of $f(x,\lambda) = 0$, $\lambda \ll 1$, are approximately described by $x_\pm \equiv x_{1,3} \sim \pm 1 + \lambda/2$ (by Taylor's expansion) and the intermediate solution is $x_i \sim -\lambda$, and for small λ,

$$c_\infty = 3\lambda/\sqrt{2} \equiv \beta\lambda.$$

The front width (Δ) is approximated as the inverse slope $[(x_+ - x_-)/x_u]$, which can be determined from $-x_{uu} = f(x,\lambda)$ by multiplying it by $2x_u$ and integrating [as in Eq. (5)] from $u=-\infty$ to 0 or $x_u^2|_0 = 2\int f(x,\lambda)dx$, where the boundaries of integration in x are x_- and $x_i \sim -\lambda$. With $\lambda \sim 0$ we find $\Delta \sim 2\sqrt{2}$. [A simpler approach for the cubic source function is to use the analytical profile, $x = \tanh(u/\sqrt{2})$.]

B. Front interaction

We want to study whether a pattern incorporating one, two, or several stationary fronts is stable and what kind of control measures can be applied to stabilize it. We show that in the absence of control the fronts are attracting or repelling each other and that global control can stabilize a single front but is unable to stabilize a multifront pattern as fronts will move in a way that maintains the setpoint.

Consider a multifront system, with fronts at $Z_1, Z_2, \ldots$, etc. In the absence of global or local control and in a uniform system we can approximate the position of all fronts and their interaction by the set of ordinary differential equation (ODE)

$$\frac{dZ_i}{dt} = \pm c(Z_{i-1}, Z_{i+1}, \lambda), \tag{14}$$

where λ is a space-independent parameter that affects the motion. A positive velocity denotes expansion of the upper state; the plus (minus) sign in Eq. (14) applies then to a front separating a high (low) state on the left from a low (high) one on the right (Fig. 1); the velocity of an ascending front is described by Eq. (13) while for that of a descending front we should exchange Z_l and Z_r. We will always assume that the first front separates a low state from a high one so that the minus/plus signs apply to fronts of odd/even numbers, when numerating the fronts from the left. Equation (14) can be written now (where $\alpha_- = \alpha_+ = \alpha$, $p_- = p_+ = p$) as

$$\frac{dZ_i}{dt} = \pm c_\infty - \alpha e^{-2pZ_l} + \alpha e^{-2pZ_r} \tag{15}$$

with positive or negative signs as before. Equation (15) is analyzed below to study front interaction by analyzing the stability of a single stationary front and of two or n such fronts, in the absence or presence of various control modes.

C. Single front

Consider now a single front solution at $z = Z_1$, separating a lower state (on the left) from a higher one. The front position is described now by Eq. (15) with $Z_r = L - Z_1$, or

$$\frac{dZ_1}{dt} = -c(Z_1, \lambda(Z_1)) = F(Z_1)$$
$$c = c_\infty + \alpha e^{-2pZ_1} - \alpha e^{-2p(L-Z_1)}. \tag{16}$$

Now, we consider the control-free system and several modes of interaction or control and analyze the system dynamics in each case.

(a) In the *absence of control* the stationary front position ($c_\infty = 0$) is unstable since $\partial F/\partial Z_1 = 2p\alpha e^{-2pZ} + 2p\alpha e^{-2p(L-Z)} > 0$ where $Z = Z_{1s}$, the stationary front position; for this symmetric case, where the front is equally attracted to the left and right boundaries $c=0$ when $Z_s = L - Z_s$ and $\partial F/\partial Z_1 = 4p\alpha e^{-pL}$. The front will move then to one of its boundaries, accelerating as the boundary is approached.

(b) We show first that in the general *perfect global-control* case ($B\to\infty$) the control may stabilize the front: The space-averaged x can be approximately determined from

$$L\langle x\rangle=(Z_1-\Delta/2)x_-(\lambda)+(L-Z_1-\Delta/2)x_+(\lambda)+\Delta\langle x_{\rm front}\rangle \tag{17}$$

while the setpoint follows, similarly,

$$Lx_s=(Z_{1s}-\Delta/2)x_-(\lambda^*)+(L-Z_{1s}-\Delta/2)x_+(\lambda^*)+\Delta\langle x_{\rm front}\rangle, \tag{18}$$

where λ^* is the set value of the parameter that induces a stationary front. Assuming $\langle x_{\rm front}\rangle=(x_++x_-)/2$ and expanding $x_\pm(\lambda)=x_\pm(\lambda^*)+(dx_\pm/d\lambda)(\lambda-\lambda^*)$, where $(dx_\pm/d\lambda)$ is evaluated along $f=0$, and subtracting the two equations we find

$$\lambda-\lambda^*=K(Z_1-Z_{1s}),$$

$$K=\frac{x_+(\lambda^*)-x_-(\lambda^*)}{Z_{1s}(dx_-/d\lambda)+(L-Z_{1s})(dx_+/d\lambda)}. \tag{19}$$

While global control operates as feedback control of the front position, the gain power declines with L in this case; since the destabilizing effect of the boundaries declines exponentially [Eq. (16)] perfect global control is sufficient to stabilize the front.

(c) Consider now the general (finite B) case of *global interaction*. In that case we need to estimate the dependence $x_\pm(\lambda)$. That may not be simple for arbitrary kinetics and we pursue it for case with *cubic kinetics:* Since $x_\pm\sim\pm1+\lambda/2$ and $L\langle x\rangle=(Z_1-\Delta/2)(-1+\lambda/2)+(L-Z_1-\Delta/2)(1+\lambda/2)+\Delta(-\lambda/2)$, where the last term is the approximate value for the front, then $\langle x\rangle=\lambda/2+1-2Z_1/L$. Thus $\lambda/2=\langle x\rangle-1+2Z_1/L$, but we also set $\lambda=B(x_s-\langle x\rangle)$, yielding

$$\lambda=\frac{B}{1+B/2}(x_s-1+2Z_1/L). \tag{20}$$

The front position is stable when $\partial F/\partial Z_1<0$, where

$$\frac{\partial F}{\partial Z_1}=-\frac{dc_\infty}{d\lambda}\frac{d\lambda}{dZ_1}+2\alpha pe^{-2pZ_1}+2\alpha pe^{-2p(L-Z_1)},$$

$$\frac{dc_\infty}{d\lambda}=\frac{3}{\sqrt{2}},\quad \frac{d\lambda}{dZ_1}=\frac{4}{L}\frac{B}{2+B}. \tag{21}$$

In the symmetric case ($x_s=0$) the front is positioned at the center, $Z_{1s}=L/2$, and

$$\frac{\partial F}{\partial Z_1}=-4\beta\frac{B}{(2+B)L}+4\alpha pe^{-pL},\quad \beta=\frac{3}{\sqrt{2}}. \tag{22}$$

(d) In *point-sensor control*, with small deviations from the setpoint, we can approximate $x(z)\sim x_f+(dx/dz)_f(z-Z_{1s})$ where $x_f=x(Z_{1s})$ is the state at the front position, dx/dz is evaluated at the front, and we have ignored changes due to the control parameter. Consequently,

$$x(Z^*)=x_f+(dx/dz)_f(Z^*-Z_1),$$

$$x_s=x_s(Z^*)=x_{fs}+(dx/dz)_{fs}(Z^*-Z_{1s}),$$

and assuming that the front shape is unchanged ($x_f=x_{fs}$, etc.), the control strategy leads to

$$A(t)=x_s-x(Z^*)=-(dx/dz)_f[Z_{1s}-Z_1],$$
$$\lambda-\lambda^*=K(Z_1-Z_{1s}),\quad K=B(dx/dz)_f, \tag{23}$$

where we usually set $Z_{1s}=Z^*$.

The gain with the point-sensor control is independent of the system length, and it can stabilize any single-front pattern of single-variable systems. Note that in the general case the actual gain depends on the sensor location, and the largest gain is achieved at the front position, where we set our sensor. Adjusting a system to a new set front position will require us to relocate the sensor location.

D. Two fronts

Consider a two-front pattern, separating domains with low, high, and low states, when numerating them along the system coordinate. The steady front positions for this symmetric case, are $Z_{1s}=L/4=L-Z_{2s}$, and the dynamics is described by

$$\frac{dZ_1}{dt}=-c_1(Z_1,Z_2,\lambda)=F_1(Z_1,Z_2,\lambda),$$
$$\frac{dZ_2}{dt}=c_2(Z_1,Z_2,\lambda)=F_2(Z_1,Z_2,\lambda),$$
$$c_1=c_\infty+\alpha e^{-2pZ_1}-\alpha e^{-p(Z_2-Z_1)},$$
$$c_2=c_\infty-\alpha e^{-p(Z_2-Z_1)}+\alpha e^{-2p(L-Z_2)}. \tag{24}$$

We consider now the dynamics of the system in the absence of control and with global interaction or control of infinite gain, showing that in both cases the steady structure described above is unstable

(a) To show that this structure is unstable in the absence of control ($\lambda=0$), we conduct a linear stability analysis of Eq. (24) to find that the Jacobian matrix

$$J=\frac{\partial(F_1,F_2)}{\partial(Z_1,Z_2)}=\alpha pe^{-pL/2}\begin{pmatrix}3 & -1\\ -1 & 3\end{pmatrix} \tag{25}$$

has positive eigenvalues. The fronts will either attract or repel each other until a homogeneous state is established.

(b) Applying perfect global control ($\langle x\rangle=x_s$, infinite B) aimed at setting $L\langle x\rangle=(Z_1-\Delta/2)x_-+(Z_2-Z_1-\Delta)x_++(L-Z_2-\Delta/2)x_-+2\Delta\langle x_{\rm front}\rangle=Lx_s$, we find that with $x_\pm=\pm1+\lambda/2$ then $\lambda=2(Lx_s+L+2Z_1-2Z_2)/L$ and

$$J=A\begin{pmatrix}-1 & 1\\ 1 & -1\end{pmatrix}+C\begin{pmatrix}3 & -1\\ -1 & 3\end{pmatrix},\quad A=\left(\frac{dc_\infty}{d\lambda}\frac{4}{L}\right),$$
$$C=(\alpha pe^{-pL/2}), \tag{26}$$

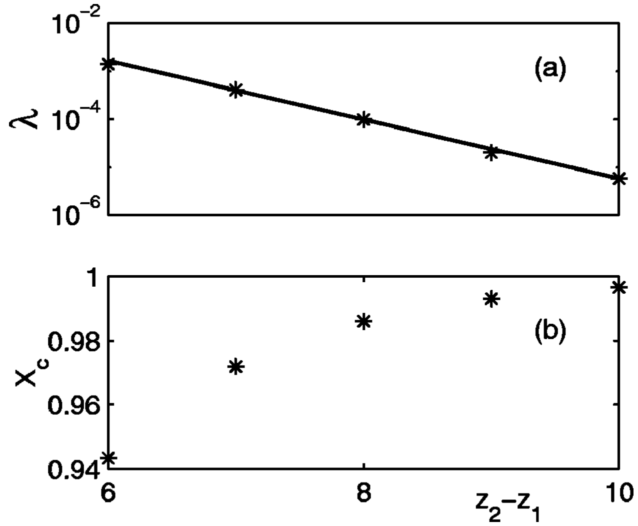

FIG. 3. The simulated (stars) and approximated λ value required for igniting a single-variable system by perturbing it in the form of a pulse (shown in Fig. 1) of size Z_2-Z_1 and the corresponding midpoint x value ($L=20$; dimensionless variables and parameters).

showing that for all set of parameters the system is unstable (its eigenvalues are $2C,\ -2A+4C$). A two-front structure cannot be stabilized in a simple way.

E. Local ignition of a cold system

A transition from the lower to the upper state (or vice versa) can be induced by applying a local perturbation in the form of a pulse. How wide should this pulse be? If we view it as two fronts, and they are a distance of $2Z$ apart in an infinitely long system, then front velocity will approximately follow Eq. (24) and we require that $c_2=c_\infty(\lambda)-\alpha e^{-2pZ}>0$, providing us with the minimal value of λ that will assure expansion of the pulse. This expression was compared with numerical results that located the boundary of an expanding and shrinking domains, after a symmetric pulse (as in Fig. 1) was imposed initially. Excellent agreement is obtained with numerical results (Fig. 3).

F. *n* fronts

The system is described now by Eq. (15) with

$$Z_l=Z_i-\frac{Z_i+Z_{i-1}}{2}=\frac{Z_i-Z_{i-1}}{2}\quad \text{except}\ \ i=1,\quad Z_1=Z_1, \tag{27}$$

$$Z_r=\frac{Z_i+Z_{i+1}}{2}-Z_i=\frac{Z_{i+1}-Z_i}{2}\quad \text{except}$$

$$i=N,\quad Z_r=L-Z_N.$$

(a) In the absence of control ($\lambda=c_\infty=0$) the stationary front positions equally divide the L size system and are described by $Z_{1s}=L/2n,\quad Z_{2s}=3L/2n,\quad Z_{is}=(2i-1)L/2n$. The Jacobian matrix of Eqs. (12) and (27) is tridiagonal with

$$\frac{J}{\alpha p e^{-pL/n}}=\begin{pmatrix} 3 & -1 & 0 & 0 & \cdot & 0\\ -1 & 2 & -1 & 0 & \cdot & 0\\ 0 & -1 & 2 & -1 & \cdot & 0\\ 0 & 0 & -1 & 2 & \cdot & 0\\ \cdot & \cdot & \cdot & \cdot & \cdot & \cdot\\ 0 & 0 & 0 & 0 & -1 & 3\end{pmatrix}. \tag{28}$$

For $n=4$, for example,

$$\frac{1}{\alpha p e^{-pL/n}}=\begin{pmatrix} 3 & -1 & 0 & 0\\ -1 & 2 & 1 & 0\\ 0 & -1 & 2 & -1\\ 0 & 0 & -1 & 3\end{pmatrix}. \tag{29}$$

A stability analysis of these systems reveals that the *n*-front stationary pattern is unstable. With time fronts will coalesce and disappear, pair by pair, until a homogeneous steady state is established.

(b) Can infinite-gain global control stabilize such a pattern? Qualitatively we know that it is impossible since the control cannot affect the motion of a pair of adjacent fronts moving in the same direction. The overall balance (for an even n) is

$$L\langle x\rangle=(Z_1-\Delta/2)x_-+(Z_2-Z_1-\Delta)x_++(Z_3-Z_2-\Delta)x_- +\cdots(L-Z_n-\Delta/2)x_-+n\Delta\langle x_{\text{front}}\rangle=Lx_s \tag{30}$$

with $x_\pm=\pm1+\lambda/2$ and $\langle x_{\text{front}}\rangle=(x_++x_-)/2$ yields

$$\frac{\lambda}{2}=x_s+1+\frac{2(Z_1+Z_3+\cdots-Z_2-Z_4-\cdots)}{L}. \tag{31}$$

When the distances between the fronts are sufficiently large the stability will depend on λ only. The system is described by $dZ_i/dt=\pm c_\infty(\lambda)$. Note that $d(Z_i+Z_{i+1})/dt=0$ and the control cannot command the separation between fronts.

Thus, a structure of n stationary fronts ($n>1$) cannot be stabilized by global control, even with sufficient separation between the front, and we expect this conclusion to hold for finite separation. In the absence of control even a single stationary front cannot be stabilized.

G. Stabilizing asymmetric fronts

Let us consider a single stationary front solution of Eqs. (1) and (2) and study the effect of varying x_s. The asymptotic solution in a large system has been outlined in several papers [22] showing that as x_s is varied the front position changes in order to maintain the setpoint but the system maintains $\lambda=0$ in order to maintain a stationary front ($c_\infty=0$). Numerical solutions for a finite system have also been outlined and the bifurcation diagram of λ vs $\langle x\rangle$ has been portrayed showing stable and unstable branches of solutions [23]. In the unstable solution the front rests close to the edge but the attraction exerted by the edge is stronger than the stabilizing effect of the controller. This control scheme has been applied in numerous studies of catalytic kinetics on thin wires in order to maintain ''isothermal'' conditions, before it was realized that this scheme leads to symmetry breaking in systems that admit bistability.

Here we want to approximate the solution to this system and find the shortest system that maintains a single stationary front. The front position is described by Eq. (16) with λ in Eq. (20) and the boundary of stability of the front is given by setting Eq. (21a) to zero. The two conditions can be written as

$$\text{(a)}\quad E^2+\frac{b}{2}(Lx_s-L+2Z_s)E-1=0,$$
$$E=e^{p(L-2Z_s)},\qquad b=\frac{4\beta}{\alpha L}\frac{B}{B+2}e^{pL},\tag{32}$$
$$\text{(b)}\quad 2pE^2-bE+2p=0.$$

Solving Eq. (32a) will yield the front position while (32b) yields the stability boundary. The latter exists only for $b^2>16p^2$, which yields the shortest system that can be stabilized, and the corresponding front position is described by $E=b/4p$.

III. CONTROL STRATEGIES

Recall that we are looking now to design a controller with as few sensors as possible and possibly with a single actuator of the form

$$\lambda-\lambda^*=BA[x(t)]\psi(z).$$

We have already tested two control strategies with uniform (homogeneous) actuators: The actual effect of both strategies on a single-front pattern can be described by

$$\lambda-\lambda^*=K(Z_1-Z_{1s})$$

[Eqs. (19) and (20)] and both strategies cannot stabilize a multifront pattern. Global control is a simple approach that is insensitive to front position but its gain (*K*) is limited in large systems. Point sensor control is another simple approach with a gain that is independent of system length but is highly sensitive to the front position.

The available controller design methods teach us how to construct a controller for multifront patterns. That typically requires several actuators. We consider now a control strategy with a *single* nonuniform (heterogeneous) actuator. This *inclination control* uses an actuator that imitates the pattern structure, i.e., the roots of $\psi(z)=0$ and the slopes of ψ are identical to those of $x_s(z)$. That will stabilize the front, if $A(t)>0$, since any front motion will be counteracted. In the inclination control of a single-front pattern let us choose $\psi(z)=H(z-Z_{1s})-1/2$, where $H(z)$ is the Heaviside function, or $\psi(z)=-\cos[\pi z/L]$. This control strategy is too elaborate for a single-front structure and is tested here mainly to apply it for multifront patterns.

Note that now λ is space dependent and we need to consider the expression for front velocity. When $\lambda(z)$ is slightly space dependent, we can expand $f(x,\lambda)=f(x,\lambda_0)+f_\lambda(\lambda-\lambda_0)$ and the front velocity in a finite but sufficiently long system is approximately

$$-c_\infty\langle x_u^2\rangle=\int_{x_-}^{x_+}f(x,\lambda_0)dx+\int_0^L f_\lambda(\lambda-\lambda_0)\frac{dx}{dz}dz,\tag{33}$$

where dx/dz is approximated from the front at λ_0. Note that, if dx/dz is an even function, as in the cubic *f* case, and for odd $\lambda(z)$, i.e., $\lambda(Z_s-z)=-\lambda(z-Z_s)$, the correction to the front velocity is nil. Note, that for $Z_{1s}=L/2$ the forcing control is an odd function and will not affect the front position.

Now, suppose the front deviates from its desired position Z_{1s} to certain Z_1 or alternately suppose that ψ is shifted relative to its steady position: Then, with the step function $\psi(z)=H(z-Z_{1s})-\frac{1}{2}$ the second term on the right of Eq. (33) is simply the integral over the displacement

$$\int_0^L(\lambda-\lambda_0)\frac{dx}{dz}dz=BA(t)\int_{Z_1}^{Z_{1s}}\frac{dx}{dz}dz=BA(t)[x(Z_{1s})-x(Z_1)]\tag{34}$$

and for small deviations the correction is $(dx/dz)_f(Z_{1s}-Z_1)$ (recall that $f_\lambda=1$ here).

Now, $A(t)$ may be chosen again to follow a global-control or a point-sensor strategy but with $A(t)>0$, e.g., $A(t)\sim[x_s-x(Z^*)]^2$, and following Eq. (32) $A(t)\sim(Z_{1s}-Z_1)^2$ and for small deviations $\lambda=BA(t)\psi(z)\sim(Z_{1s}-Z_1)^3$. While this term will not affect the linear stability analysis it will affect the motion and arrest the front when the cubic term is comparable to the linear one. To analyze this situation note that there usually exists a destabilizing force, which for small deviations is of the linear form $\nu(Z_{1s}-Z_1)$. [The destabilizing force is either due to edge effects, Eq. (16), or due to other effects such as a localized inhibitor as we will demonstrate in Sec. IV.] The stabilizing force, from Eq. (34), is of the form $Bb(Z_{1s}-Z_1)^3$, where *b* is a constant $[\sim(dx/dz)_f^2]$. Thus

$$\frac{d(Z_{1s}-Z_1)}{dt}=c=\nu(Z_{1s}-Z_1)-Bb(Z_{1s}-Z_1)^3.\tag{35}$$

Simple inspection shows that the desired solution $Z_1=Z_{1s}$ is unstable, but there exists another solution at $(Z_{1s}-Z_1)^2=\nu/Bb$, with a corresponding $\lambda=Bb(Z_{1s}-Z_1)^3$ $[=\nu^{3/2}/(Bb)^{1/2}]$ which is stable. This approach leads, therefore, to a different steady-state profile, but with increasing gains (*B*) the difference between these steady states diminishes $(Z_{1s}-Z_1\to0,\lambda\to0)$.

These results were verified by simulations of the full reaction-diffusion equation (1a) subject to control [Eq. (3)] with $\psi(z)=H(z-Z_{1s})-1/2$ starting with a small perturbation to the front solution. The simulations [Fig. 4(a)] show that indeed the front is arrested by the control, and the process is faster with larger gain (B), but the corresponding front position (Z_f) and λ deviate slightly $(10^{-2}$ to $10^{-3})$

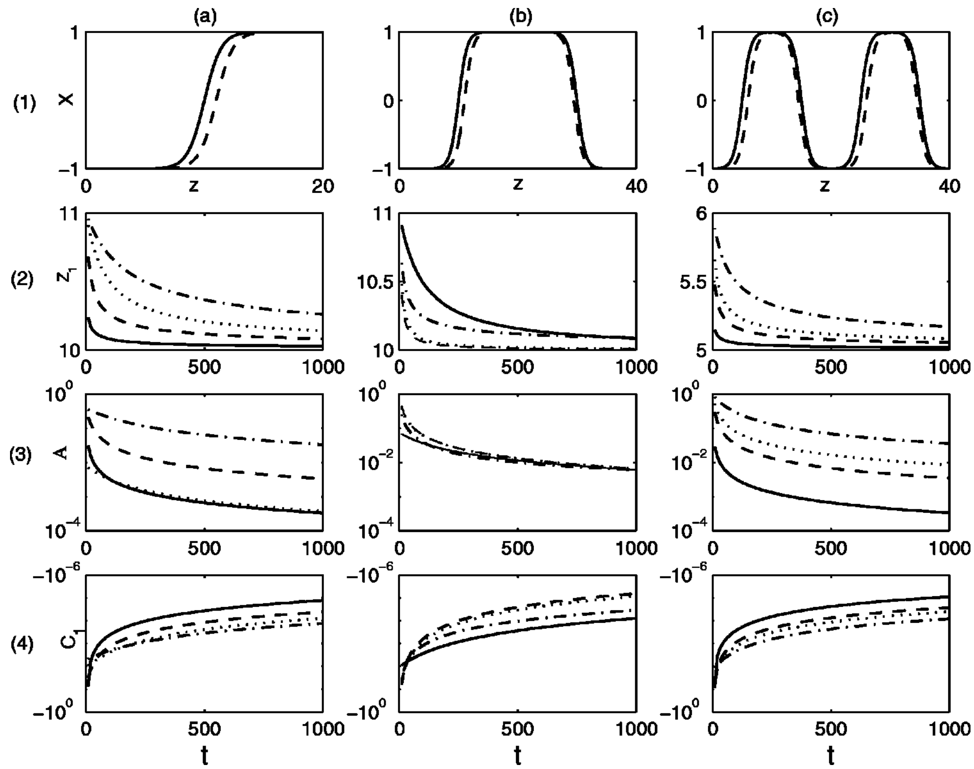

FIG. 4. Stabilizing a one- (a), two- (b), and four-front (c) pattern ($L=20$, 40, and 40, respectively) in a single-variable model using a single space-dependent Heaviside form actuator Ψ. Simulations show the stationary and perturbed patterns (first rows, solid and broken lines) and the response to a small perturbation of the left-front position (Z_1, second row), the control value (third row), and the front velocity (fourth row). (Various lines present the comparison of various control parameters. Diagram (2) presents the effect of B with 0.01 (dash-dotted line), 0.1 (broken line), and 1.0 (solid line) with a sensor positioned at the front ($Z=10$) or $B=0.1$ and sensor at $Z=8$ (dotted line). Diagram (3) shows the effect of the control mode [Eqs. (37a) (solid line), (37b) (broken line), (37c) (dash-dotted line), and (37d) (dotted line), $B=1.0$]. Diagram (4) shows the effect of B, the notation as in (a)) (dimensionless variables and parameters).

from the desired values of the unstable stationary front (where λ should be nil). The difference between the setpoint and the new front is not noticeable. Placing the sensor somewhat away from the desired front position (at $z=8$ instead of 10) will result in a slower convergence, but the system will approach the same solution.

While some of the methods described earlier can control a single front in its position, they may not work with a two- or n-front pattern. Global control was shown already to be unsuccessful for this task [Eq. (22)]. For a two-front pattern we may opt to choose one of the following forms, a square wave or a cosine function:

$$\text{(a)}\quad \psi=[H(z-Z_1^*)H(Z_2^*-z)-\tfrac{1}{2}],\qquad \text{(b)}\quad \psi=-\cos(2\pi z/L). \tag{36}$$

As we show this approach will not be able to stabilize the desired pattern, for the reasons described above for a single-front pattern, but may yield a sufficiently close solution. $A(t)$ should be positive definite and should be sensitive to motions of all fronts, e.g.,

$$A(t)=\langle (x-x_s)\psi(z)\rangle, \tag{37a}$$

$$A(t)=|x(Z_1^*)-x_{1s}|+|x(Z_2^*)-x_{2s}|, \tag{37b}$$

$$A(t)=[x(Z_1^*)-x_{1s}]^2+[x(Z_2^*)-x_{2s}]^2, \tag{37c}$$

$$A^2(t)=[x(Z_1^*)-x_{1s}]^2+[x(Z_2^*)-x_{2s}]^2, \tag{37d}$$

where Z_1^* denotes sensors location. Equation (37a), where $\langle\ \rangle$ denotes integration over the system, may not be sufficient as the motion of both fronts will cancel their individual effects. Equations (37b)–(37d) require two local sensors in the vicinity of the desired front position, Z_{1s},Z_{2s}. Equation (37b) is not continuous in its derivatives and Eq. (37c) yields a quadratic response and thus will affect the motion only at large deviations but will not affect the linear stability analysis. This was shown for a single front and can be shown to apply for the other control options above as well. The approximate analysis can be conducted by reducing the model to describe the front position. In that case, control schemes (37b)–(37d) above should be transformed to

$$\text{(b)}\quad A(t)\sim|Z_1-Z_1^*|+|Z_2-Z_2^*|,$$
$$\text{(c)}\quad A(t)\sim(Z_1-Z_1^*)^2+(Z_2-Z_2^*)^2, \tag{38}$$
$$\text{(d)}\quad A^2(t)\sim(Z_1-Z_1^*)^2+(Z_2-Z_2^*)^2.$$

Similar $\psi(z)$ and $A(t)$ functions will be constructed for other n-front patterns.

Simulations of the system, subject to space-dependent actuators [Eq. (37)], starting with small perturbations to two- and four-front structures [Figs. 4(b) and 4(c)] show that indeed the desired state is unstable but that it can usually be achieved with a reasonable accuracy. The choice of the control mode is not important and with increasing gain the response is faster but the deviation from the desired state is larger.

IV. ACTIVATOR INTERACTION WITH A LOCALIZED INHIBITOR

We consider now the behavior of a two-variable system, incorporating a fast activator (x) and a slow nondiffusing inhibitor (y) described by Eq. (1b). This problem has been investigated extensively since it describes various physical systems as low- and high-pressure catalytic reactions (see [12] for a recent review) and neural conduction. Front dynamics, in systems with a wide separation of time scales ($\varepsilon \ll 1$), can be studied, to a first approximation, by assuming that the inhibitor position is frozen. This may destabilize the front position as explained below. Much of the analysis conducted above can be applied now for the two-variable (x,y) system. Under global control, however, where the system is forced to admit a preset space-averaged value, $\langle x \rangle = x_s$, a plethora of patterns may emerge [15]; some of these patterns were observed in catalytic, electrochemical, and gas-discharge systems [12]. The shape of stationary fronts is different from those in single-variable systems, since the inhibitor has ample time to relax and affect the front shape. The transition from stationary to moving fronts was described in several works and may be associated with a hysteresis loop [24]. For $\varepsilon \ll 1$, however, the transition is fast and we can apply the results outlined above.

For simplicity we assume a linear $g(x,y)$

$$g(x,y) = -\gamma x - y. \tag{39}$$

A simple analysis of the homogeneous steady states of Eqs. (1a) and (1b) with the specified kinetics reveals bistablity with two stable solutions when $\gamma < \frac{2}{3}$ and a unique unstable state for $\gamma > 1$; bistability exists also for $\frac{2}{3} < \gamma < 1$ but their stability depends on ε. Stationary front solutions exists for $\gamma < 1$ but they are unstable for $\gamma > \varepsilon$. These fronts separate two stable states when $\gamma < \frac{2}{3}$, and their stabilization is relatively simple, while for $\frac{2}{3} < \gamma < 1$ the limiting states may be unstable. We focus our attention, therefore, on the former case. The latter case will be addressed elsewhere using a formal control approach [25].

Single-front dynamics

For a *moving front*, and for sufficiently short times for which the $y = y_s$ profile can be assumed to be frozen at the steady-state value, we can apply the analysis conducted above. For the specific model used here λ and y have the same effect on the front position, so that for a front separating low (on its left) and high states, we find

$$x_{\pm} = \pm 1 + (\lambda + y_{sf})/2, \quad \lambda + y_{sf} = 2(Lx_s - L + 2Z_1)/L,$$

$$c_\infty = \beta(\lambda + y_{sf}), \tag{40}$$

where y_{sf} is the local value at the front position and the effect of gradients in y_s on the front velocity are ignored. The ''frozen'' y profile is its steady-state profile, and following the steady x profile it will be divided into three sections: At the outer sections $y_{\pm} = -\gamma x_{\pm}$ while at the inner section the front slope at its inflection point is $dx/dz|_0 = \Delta = (1-\gamma)\sqrt{2}$ and consequently $dy_s/dz|_0 = -\gamma(1-\gamma)\sqrt{2}$.

(a) In an uncontrolled system, described by $dZ_1/dt = -c(Z_1, y)$, the stationary front ($c=0$) is unstable since

$$\frac{\partial F}{\partial Z_1} = -\frac{\partial c}{\partial Z_1} = \frac{\partial c}{\partial y}\left.\frac{\partial y_s}{\partial Z}\right|_0 + 2p\alpha e^{-pL} \tag{41}$$

and both terms are positive.

(b) For a very long system, for which attraction by the boundaries can be neglected, the front position is described by

$$dZ_1/dt = -c_\infty = -\beta[\lambda(Z_1) + y_s(Z_1)]. \tag{42}$$

Under *global control* with infinite gain the system is stable when

$$\frac{\partial c_\infty}{\partial Z_1} = \beta\left(\frac{\partial \lambda}{\partial Z_1} + \left.\frac{\partial y_s}{\partial z}\right|_{Z_1}\right) = \beta\left(\frac{\beta}{L} - \gamma\frac{1-\gamma}{\sqrt{2}}\right) > 0. \tag{43}$$

Obviously global control is efficient only in short systems.

The effect of *point-sensor control* is expressed in Eq. (23) and the front will be stable when

$$K - \gamma(1-\gamma)\sqrt{2} > 0. \tag{44}$$

Thus, a single-front that connects two stable state (i.e., $\gamma < \frac{2}{3}$) can be easily stabilized by a single point-sensor control. This result was verified by computing the corresponding eigenvalues. More sensors are required when $\gamma > \frac{2}{3}$ and their number increases with γ; the control design in this case requires a formal approach, as we outline in a future work.

(c) *Multifront patterns* cannot be controlled by a single sensor and a single actuator. An n-front pattern can be easily controlled by n space-dependent actuators, each responding to a sensor located at the front position and affecting its immediate vicinity. An n-front pattern can be approximately controlled by a single space-dependent actuator [Eqs. (36) and (37)] that responds to the sum of the deviation of n sensors; the adequacy of the approximation depends on the problem and parameters and requires some optimization of the control gain. One such example is shown in Fig. 5 which portrays the response to small perturbations in simulations of the full system [Eqs. (1a) and (1b)] subject to control of Eqs. (3) and (37c) with ψ that is either a Heaviside product [Eq. (36a), the solid line in the top of Fig. 5] or a modified discontinuous function (the broken line in the top figure) that affects the front vicinity but its impact away from the front is diminishing. Figure 5 plots the midpoint activator value

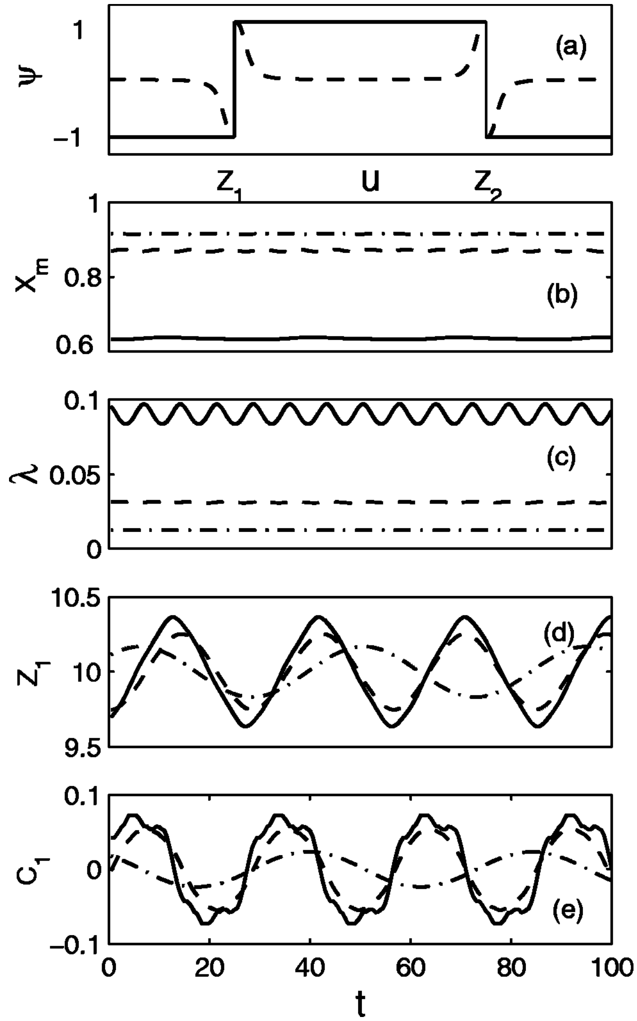

FIG. 5. Stabilizing a pulse pattern ($L=40$) in a two-variable model using a single space-dependent actuator [ψ, presented in (a), is a Heaviside product function as in Eq. (36a), solid line, or a modified function, broken line]: simulation results show the state at midpoint (b), the control value (c), the left-front position (d), and the front velocity (e) following a perturbation to the initial steady state. [$B=10$ and $\gamma=0.3$ (dash-dotted line) and 0.6 (broken line) with ψ as a Heaviside function, and $\gamma=0.6$ with modified ψ (solid line); dimensionless variables and parameters.]

$x(0)$, the control effect, the left-front position, and its velocity for $\gamma=0.3$ and 0.6 (Heaviside control, dash-dotted and broken lines) and $\gamma=0.6$ with the modified function (solid line). While all control modes induce small oscillations in position and small time-averaged values of λ, the modified function yields more accurate results as evident from the midpoint value.

V. CONCLUDING REMARKS

We have analyzed the stability of one-dimensional patterns in reaction-diffusion systems by analyzing the interaction between adjacent fronts and between fronts and the boundaries in bounded systems. We have used model reduction to a presentation that follows the front positions, while using approximate expressions for front velocities, in order to study various control modes in such systems. These results were corroborated by few numerical experiments.

The analysis of a single-variable model showed that a single front or a pattern with n fronts is typically unstable, due to the interaction with the walls. Two simple control modes based on a single sensor and a single spatially homogeneous actuator were analyzed: Global control may or may not stabilize such front while a point-sensor control (pinning) will arrest this front. Both control modes, in fact, respond to front position. Neither of these control modes can stabilize an n-front pattern and that task calls for a distributed actuator. While a multipoint controller that incorporates n sensors, each signaling a controller that affects the vicinity of the corresponding front, can stabilize such a pattern, this may be technically too complex. A single space-dependent actuator that responds to the sum of deviations in the front positions may stabilize a pattern that approximates the desired state. The deviation between the two may be sufficiently small to render the obtained state satisfactory.

The interaction of an activator with a nondiffusing and slow inhibitor, in a two-variable model, leads to a destabilizing effect and poses an even larger challenge for stabilizing stationary patterns. Such interaction may lead to bistability or oscillations in a lumped system. For conditions that induce a stable moving front in an uncontrolled system (which correspond to bistability in a lumped system), a global-control approach is effective for arresting a single front only in short systems, while in long ones a pulse motion will emerge. Point-sensor control is effective for this task for any size of the system. Both approaches fail to stabilize an n-front pattern, but the distributed actuators described above may be effective in this case.

The methodologies developed here can be extended to other models that incorporate patterns. In a future application we will consider the control of moving fronts; these are of importance in several physiological systems, most notably in cardiac systems (e.g., [26]). Stationary fronts may appear in catalytic fixed bed reactors, which are described by reaction-diffusion-convection systems [12]. Convection affects the front velocity as it ''pushes'' the front downstream. In a recent work [11] we studied the stabilization of a stationary pattern in a simple homogeneous model of a tubular catalytic reactor with generic first-order exothermic reaction and realistic Pe values (the ratio of convection to diffusion terms) and subject to realistic boundary conditions. To admit homogeneous solutions we considered in that work a reactor model that admits local bistability due to the interaction of nonlinear kinetics (due to exothermic and activated reaction) with heat loss due to cooling, and with a mass generation source, either by the preceding reaction or by mass supply through the membrane wall (see [16] for a detailed description). Linear stability analysis combined with the Galerkin method was used for state feedback control of the distributed parameter system. The capabilities of the global control and point-sensor control to stabilize the front solution were studied by the manipulation of various reactor parameters including fluid flow and feed conditions. Point-sensor control of the coolant flow (heat-loss coefficient) or coolant temperature are the most effective when the temperature sensor is located close to the front position. Global control and other strategies failed. A qualitative analysis was suggested for the selection of proper control of front stabilization and it follows the principles presented here, as we discuss below.

The full model studied by Panfilov and Sheintuch [11] is too complex for a detailed analysis. The qualitative analysis presented there is based on the reduction of the original PDE model to a simple ODE that describes the front position, using an approximate expression for the front velocity. Thus, the enthalpy and mass balances were argued to be linearly related and qualitatively described by an equation of the following form:

$$x_t + \mathrm{Pe}\, x_z - x_{zz} = f(x,y,p^*) + f_p(p-p^*),$$
$$z=0, \quad x_z = \mathrm{Pe}\, x; \quad z=L, \quad x_z=0, \tag{45}$$

where x (the temperature) is the activator and the inhibitor (y) is qualitatively described by Eq. (1b); they have singled-out the effect of a parameter (p) to be used for control purposes. As we reviewed here, certain analytical results exist for the front velocity in the unbounded diffusion-reaction system of the form $x_t - x_{zz} = f(x)$, with an S-shaped source function and constant parameters. To apply these results to Eq. (45) we need to correct the front velocity for the convective (or rather advective) flow and for the finite-size and the boundary conditions. The edge effects on the front velocity decay exponentially with the front distance from the edges [Eq. (10)], and for the sake of simplicity we assume that the separation is sufficiently large to ignore it. Under these conditions we focus on the effect of the parameter p on the front velocity, which can be shown to be described by

$$dZ/dt = -c = -c(\mathrm{Pe}=0) + \mathrm{Pe}. \tag{46}$$

Thus, the front velocity is affected by any parameter that affects the velocity in the absence of convection and by the convection velocity. These effects can be analyzed using the tools developed above.

ACKNOWLEDGMENTS

This work was supported by the Israel Science Foundation and the U.S.–Israel Binational Science Foundation. M.S. is a member of the Minerva Center for Physics of Complex Systems.

[1] C. Georgakis, R. Aris, and N. R. Amundson, Chem. Eng. Sci. **32**, 1359 (1977).

[2] S. V. Shvartsman and I. G. Kevrekidis, AIChE J. **44**, 1579 (1998).

[3] P. D. Christofides and P. Daoutidus, Comput. Chem. Eng. **20**, S1071 (1996).

[4] F. J. Doyle, H. M. Budman, and M. Morari, Ind. Eng. Chem. Res. **35**, 3567 (1996).

[5] P. D. Christofides and P. Daoutidus, Chem. Eng. Sci. **53**, 85 (1998).

[6] W. H. Ray, *Advanced Process Control* (McGraw-Hill, New York, 1981).

[7] V. Panfilov and M. Sheintuch, Chaos **9**, 78 (1999).

[8] D. A. Jones and E. S. Titi, SIAM (Soc. Ind. Appl. Math.) J. Math. Anal. **25**, 894 (1994).

[9] H. Fife, *Mathematical Aspects of Reaction and Diffusing Systems* (Springer, Berlin 1979).

[10] A. S. Mikhailov, *Foundation of Synergetics I. Distributed Active Systems* (Springer-Verlag, Berlin, 1990).

[11] V. Panfilov and M. Sheintuch, AIChE J. **47**, 196 (2001).

[12] M. Sheintuch and S. Shvartsman, AIChE J. **42**, 1041 (1996).

[13] O. Lev, M. Sheintuch, L. M. Pismen, and H. Yarnitski, Nature (London) **338**, 458 (1988).

[14] M. Sheintuch, Chem. Eng. Sci. **44**, 1081 (1989).

[15] U. Middya, M. D. Graham, D. Luss, and M. Sheintuch, J. Chem. Phys. **98**, 2823 (1993).

[16] O. A. Nekhamkina, A. A. Nepomnyaschchy, B. Y. Rubinstein, and M. Sheintuch, Phys. Rev. E **61**, 2436 (2000).

[17] U. Middya, D. Luss, and M. Sheintuch, J. Chem. Phys. **100**, 3568 (1994).

[18] M. Sheintuch, Physica D **102**, 125 (1997).

[19] U. Middya and D. Luss, J. Chem. Phys. **102**, 5029 (1995).

[20] M. Sheintuch and O. Nekhamkina, J. Chem. Phys. **107**, 8165 (1997).

[21] M. C. Cross and P. C. Hohenberg, Rev. Mod. Phys. **65**, 961 (1993).

[22] L. M. Pismen, Chem. Eng. Sci. **35**, 1950 (1980).

[23] M. Sheintuch and J. Schmidt, Chem. Eng. Commun. **44**, 33 (1986).

[24] A. Hagberg and E. Meron, Nonlinearity **7**, 805 (1994).

[25] Y. Smagina, O. Nekhamkina, and M. Sheintuch, Ind. Eng. Chem. Res. (to be published).

[26] J. Qu, J. N. Weiss, and A. Garfinkel, Phys. Rev. Lett. **78**, 1387 (1997).